JJCO Japanese Journal of Clinical Oncology

Jpn J Clin Oncol 2013;43(6)654–663
doi:10.1093/jjco/hyt055
Advance Access Publication 16 April 2013

The Clinical Significance of Breast MRI in the Management of Ductal Carcinoma *In Situ* Diagnosed on Needle Biopsy

Minoru Miyashita[1,2,*], Goro Amano[1], Takanori Ishida[2], Kentaro Tamaki[2], Fumiaki Uchimura[3], Tomo Ono[3], Mioko Yajima[4], Yoshiki Kuriya[1] and Noriaki Ohuchi[2]

[1]Department of Surgery and Breast Surgery, Nihonkai General Hospital , Sakata, [2]Department of Surgical Oncology, Graduate School of Medicine, Tohoku University, Aoba-ku, Sendai, [3]Department of Radiology, Nihonkai General Hospital and [4]Department of Pathology, Nihonkai General Hospital, Sakata, Japan

*For reprints and all correspondence: Minoru Miyashita, Department of Surgery and Breast Surgery, Nihonkai General Hospital, 30 Akiho-cho, Sakata 998-8501, Japan, and Department of Surgical Oncology, Graduate School of Medicine, Tohoku University, 1-1 Seiryo-machi, Aoba-ku, Sendai 980-8574, Japan. E-mail: atihsayim8m8@med.tohoku.ac.jp

Received November 15, 2012; accepted March 25, 2013

Objective: To identify the factors associated with invasive disease in ductal carcinoma *in situ* diagnosed on needle biopsy by analyzing breast magnetic resonance imaging findings with the histopathological factors of biopsy specimens.

Methods: This was an institutional review board-approved, Health Insurance Portability and Accountability Act-compliant study. Seventy-five ductal carcinoma *in situ* patients diagnosed by needle biopsy who underwent preoperative magnetic resonance imaging were retrospectively reviewed. The magnetic resonance imaging and histopathological variables were assessed between pure ductal carcinoma *in situ* and invasive breast cancer diagnosed on surgical specimens. Multivariable analyses were performed to determine the independent factors for invasion using a logistic-regression model.

Results: The median age of patients was 55 (34–76) years. On dynamic magnetic resonance imaging, 60 cases out of 75 (80%) were classified as non-mass-like enhancement type and 15/75 (20%) were Mass type. In non-mass-like enhancement, 11/60 (18%) were ultimately diagnosed as invasive breast cancer. Lesion size ($P = 0.027$), signal intensity ratios (calculated as the signal intensity of detected lesions divided by the signal intensity of surrounding normal breast tissue; $P = 0.032$) on magnetic resonance imaging and the number of biopsy-cores containing cancer nests ($P = 0.012$) were each independently associated with invasion. Furthermore, each signal intensity ratio of invasive and non-invasive components of invasive breast cancer represented a value significantly higher than that of 49 pure ductal carcinoma *in situ* classified as non-mass-like enhancement ($P = 0.001$ and $P = 0.034$, respectively). Conversely, there were no significant magnetic resonance imaging findings to distinguish seven invasive breast cancer from among Mass type.

Conclusions: Needle-biopsy-proven ductal carcinoma *in situ* cases with non-mass-like enhancement type might be sufficiently managed using breast magnetic resonance imaging features such as enhanced lesion size and signal intensity, incorporating the number of cancer-cores at needle biopsy specimen in the clinical setting.

Key words: MRI – breast cancer – DCIS – occult invasion – needle biopsy

INTRODUCTION

According to previous studies, 8–38% of ductal carcinoma *in situ* (DCIS) cases diagnosed on needle biopsy have invasive disease in the surgical specimens, which require surgical staging of the axillary lymph nodes (1–9). Therefore, when planning a surgical strategy for treating preoperatively diagnosed cases of DCIS, it is clinically important to be able to more accurately predict the presence or absence of unexpected invasive disease in surgical specimens. While several images and clinicopatholgical factors are reportedly correlated with the upstage determined on final diagnosis, there is controversy regarding which subgroups should be indicated for sentinel lymph node biopsy (SLNB) at the same time as breast operation (4–9).

In recent years, breast magnetic resonance imaging (MRI) has been recommended as a modality with higher sensitivity for detecting DCIS and greater accuracy for depicting the extent of diseases (10–14). DCIS often appears as a non-mass area with clumped internal enhancement in segmental or ductal distributions using the breast imaging-reporting and data system (BI-RADS) MRI lexicon (15–17). However, the specific features of MRI that are associated with the upstage of invasive disease in cases of preoperatively diagnosed DCIS are not yet clearly described. Therefore, further examination of MRI findings in these situations is necessary and may contribute to improving the clinical management of DCIS patients. Regarding the evaluation of MRI, a sufficient biopsy of breast lesions is important as well in order to prevent the underestimation of disease. Because the accuracy of preoperative diagnoses is greatly affected by sampling errors, the factors related to the sampling procedure should be assessed objectively. However, to the best of our knowledge, little information concerning these factors has been previously reported in the literature. For this reason, the assessment of MRI and histopathological factors incorporating the status of needle biopsy specimens together is thought to be essential for improving the treatment of DCIS patients.

Our aim was to identify the factors associated with invasive disease in DCIS diagnosed on needle biopsy by analyzing breast MRI findings with the histopathological factors of biopsy specimens.

PATIENTS AND METHODS

Patients

Eighty-three consecutive female patients preoperatively diagnosed with DCIS in our institution from April 2008 to March 2012 were retrospectively identified. We excluded four patients diagnosed by surgical biopsy and four patients who had no preoperative breast MRI because they should obviously undergo mastectomy due to the multicentric cancers detected on ultrasound. Finally, 75 of 83 who were diagnosed by needle biopsy and routinely underwent preoperative MRI were eligible for this study. Clinical information was reviewed through the database of the hospital. Our institutional review board approved the protocol of this study, and all of the procedures in the management of breast cancer were based on informed consent.

All the patients received physical examinations, diagnostic mammography and ultrasound. Ultrasound-guided core-needle biopsy (ACECUT, 16-gauge; TSK Laboratory, Japan) and vacuum-assisted biopsy (Mammotome, 11-gauge; Ethicon Endo-Surgery, Cincinnati, OH, USA) could be performed in 47 and 11 patients, respectively, because the breast lesions could be detected on ultrasound due to comparatively smaller breasts of Asian females. Seventeen patients underwent stereotactic vacuum-assisted biopsy (Mammotome, 11-gauge; Ethicon Endo-Surgery), because no abnormal findings were detected on ultrasound.

MRI Protocol and Interpretation

All breast MRI was performed on a 1.5 T system (Symphony; Siemens Medical Solutions, Erlangen, Germany). The imaging protocol consisted of fat-suppressed T2-weighted (FS-T2W) image followed by dynamic-enhanced series. The FS-T2W image was obtained with the following parameters: TR/TE = 7700/77 ms, field of view (FOV) = 20 cm, 4.0-mm slice thickness, 256 × 256 matrix size and number of excitation (NEX) 3. Dynamic MRI was imaged before and four times (at 60, 120, 180 and 240 s) after a bolus injection of 0.2 ml/kg body weight of Gd–DOTA (Magnescope, Guerbet, Japan) and 20 ml of saline using a power injector. The parameters of this series included TR/TE/FA = 4.9/2.0/25 ms, FOV = 20 cm, 0.9-mm slice thickness, 256 × 256 matrix size and NEX 3.

The MRIs were interpreted by well-trained radiologists (with 26–30 years of experience) without information regarding findings of other imaging modalities or histological results of biopsies. The morphological features were assessed using the American College of Radiology BI-RADS MRI lexicon (15). For the kinetic analysis, we set region of interest (ROI) on the most enhanced area and evaluated the enhancement pattern using institutional software. The shape of the kinetic curve was categorized into three initial-phase patterns (slow, medium and rapid) at the first 120 s and three delayed-phase patterns (persistent, plateau and washout) according to the BI-RADS MRI lexicon (15). All MRI evaluations incorporating lesion size and location were recorded into our database.

For the additional study, we measured the signal intensity (SI) of detected breast lesions and surrounding normal breast tissue on dynamic MRI and calculated the SI ratio as the SI of detected lesion divided by that of surrounding normal breast tissue. The SI of detected breast lesions was defined as the maximum value of SI by placing ROIs on the whole enhanced area, because some cases have heterogeneous enhanced patterns, and that of surrounding normal breast tissue was SI of non-enhanced surrounding area without information regarding the site of cancer on dynamic MRI

obtained 120 s after the administration of contrast material. We also calculated each SI ratio of non-invasive and invasive components separately in invasive breast cancer (IBC). In this analysis, we excluded patients in whom the proportion of non-invasive nests in the entire lesion was not large enough to measure the SI of the non-invasive component. The procedure was as follows: first, we overlapped the maximum intensity projection (MIP) images with the histopathological mappings of surgical specimens by using imaging software. Next, we divided the cancerous lesions into portions of pure non-invasive components and portions containing invasive carcinomas on MIP images with reference to the histopathological mappings. Then, we detected each original slice of dynamic MRI matched either up to non-invasive or up to invasive portions. Finally, using the two different slices and portions of original dynamic MRI, we calculated each SI ratio of non-invasive and invasive lesions separately for analysis (Fig. 1).

Histopathological Analysis

The needle biopsy specimens were formalin-fixed, paraffin-embedded and cut into 4-μm-thick sections and stained with hematoxylin–eosin for histopathological examinations. First, the number of sampled cores (sample-cores) and the number of cores containing cancer nests (cancer-cores) were counted in each individual case. The degree of DCIS was categorized as 1 (low), 2 (intermediate) or 3 (high) nuclear grade (NG), and the presence or absence of comedo necrosis (CN) was determined. Additional immunohistochemistry (IHC) of

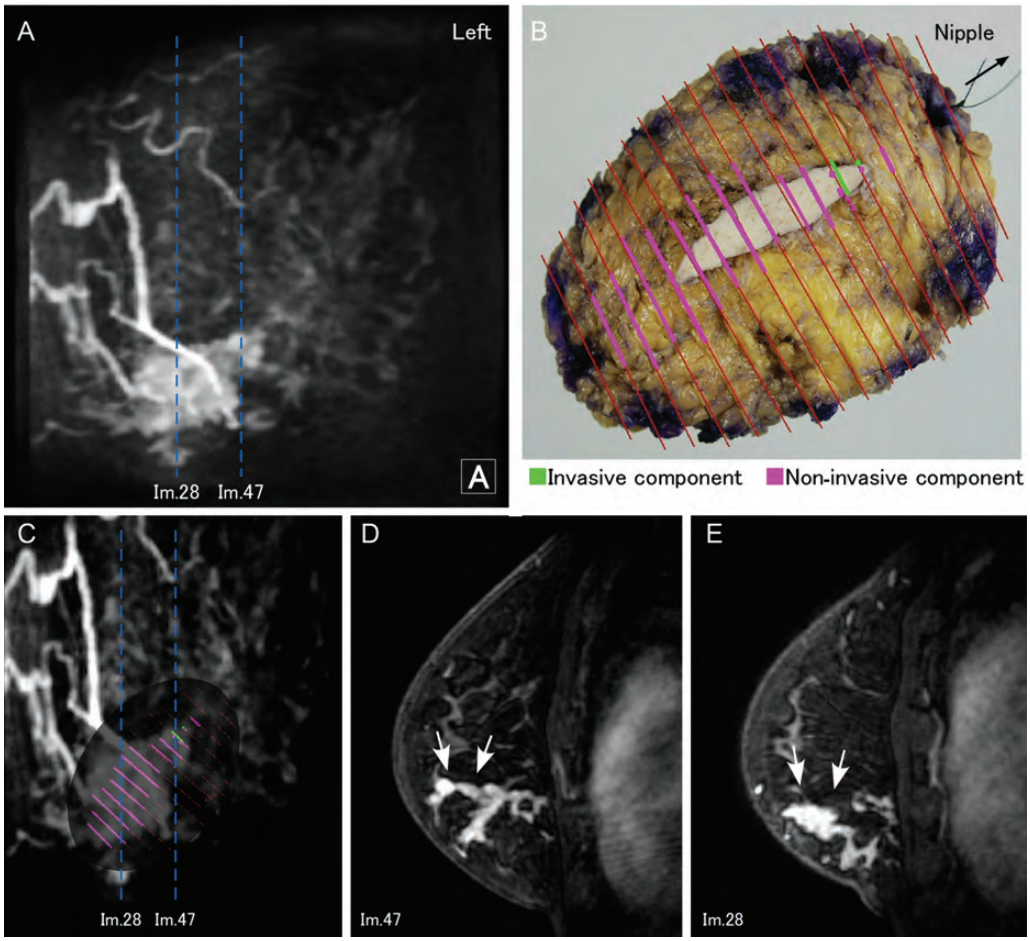

Figure 1. (A) The anterior view of maximum intensity projection (MIP) image obtained with dynamic magnetic resonance imaging (MRI). The blue dashed lines indicate the original slices (Im.28 and Im.47) of dynamic MRI. (B) The histopathological mapping of the surgical specimen with serial sections of 5 mm thickness (red lines). The stitch shows the direction of the nipple. The green and pink markers show the invasive and non-invasive components, respectively. (C) The MIP image overlapped with the histopathological mapping by using the imaging software. The blue dashed line named Im.47 indicates the original slice (Im.47) matched up to the invasive component presented as green marker on the histopathological mapping, and the blue dashed line named Im.28 indicates the slice matched up to the non-invasive component (pink marker). (D) The sagittal enhanced image (Im.47) matched up to the invasive component. Arrows indicate the enhancement legion partly containing the invasive disease. (E) The sagittal enhanced image (Im.28) matched up to the non-invasive component. Arrows indicate the enhancement legion of the non-invasive component, not containing the invasive disease. These MR images were obtained 120 s after the administration of contrast material. We calculated each signal intensity (SI) ratio of the non-invasive and invasive components separately in the invasive breast cancer (IBC) cases using the two different slices (Im.28 and Im.47) and portions (arrows) of the original dynamic MRI (D, E).

myoepithelial markers (cytokeratin 5/6, p63 and CD10) was performed for confirming the absence of microinvasion and estrogen receptor, progesterone receptor and human epidermal growth factor-receptor 2 for evaluating the biology of carcinoma. The surgical specimens of both breast-conserving surgery and mastectomy were cut into serial sections of 5 mm thickness. The final diagnoses of non-invasive or invasive disease were made using IHC of the above-mentioned myoepithelial markers. All the histopathological diagnoses and staining assessments were performed by two authors, one of whom is an expert in breast pathology.

Statistical Analysis

The MRI findings and clinicopathological factors of each group were compared using Fisher's exact test and the χ^2 test when factors were categorical variables. The continuous variables were compared using Student's *t*-test and the Wilcoxon rank-sum test. Multivariate analysis using a logistic-regression model was performed to determine the factors associated with invasion. For these factors, the cutoff values to distinguish between IBC and DCIS were examined using receiver operating characteristic (ROC) curves, and the predictive values, such as sensitivity and specificity, were calculated. All the statistical analyses were completed using JMP 9.0.2 (SAS Japan, Tokyo, Japan). A P value of <0.05 was considered to be statistically significant.

RESULTS

We evaluated 75 DCIS patients diagnosed by needle biopsy for this study. The median age of the patients was 55 (range: 34–76) years. In 12 cases, there were positive findings on physical examination. The median lesion size was 10 (range: 0–79) mm on mammography and 8 (range: 0–45) mm on ultrasound. On breast MRI, 60 cases of 75 (80%) were classified as non-mass-like enhancement (NMLE) type, 15/75 (20%) were classified as Mass type and the median lesion size was 16 (range: 5–60) mm. The median number of sample-cores and cancer-cores was four (range: 1–13) pieces and three (range: 1–10) pieces, respectively. According to the results of the needle biopsies, 59 cases of 75 (79%) were Grade 1 in NG, 9/75 (12%) were Grade 2 and 7/75 (9%) were Grade 3, and CN was observed in 41 cases of 75 (55%).

Based on the advanced search of the surgical specimens, 57 cases of 75 (76%) were ultimately diagnosed as pure DCIS and invasive components existed in 18/75 (24%) cases that were preoperatively considered to be DCIS. In all patients who received SLNB at the time of surgery, there was no metastatic cancer in sentinel lymph nodes. The results of comparing the clinicopathological factors and image findings of the DCIS group and the IBC group are summarized in Table 1. Among the two groups, there were significant differences in lesion type on MRI (NMLE or

Table 1. Patient characteristics according to the final diagnoses, pure DCIS or IBC group

Variables	DCIS ($n = 57$)	IBC ($n = 18$)	P value
Age (years)			0.217
Median	55	52	
Range	34–76	39–71	
Physical examination			0.021
Positive	6	6	
Negative	51	12	
Lesion size on mammography (mm)		0.895	
Median	10	11	
Range	0–79	0–66	
Lesion size on ultrasound (mm)			0.066
Median	7	10	
Range	0–35	3–45	
Lesion size on MRI (mm)			0.165
Median	15	17	
Range	5–60	6–59	
MRI lesion type			0.022
Mass	8	7	
NMLE	49	11	
The number of sample-cores			0.108
Median	5	3	
Range	2–12	1–13	
The number of cancer-cores			0.002
Median	3	2	
Range	1–10	1–7	
Nuclear grade			0.839
1 (low)	45	14	
2 (intermediate)	7	2	
3 (high)	5	2	
Comedo necrosis			0.931
Positive	31	10	
Negative	26	8	
Estrogen receptor status			0.787
Positive	46	14	
Negative	11	4	
Progesteron receptor status			0.386
Positive	41	11	
Negative	16	7	
HER2 status			0.344
Positive	10	5	
Negative	47	13	

DCIS, ductal carcinoma *in situ*; IBC, invasive breast cancer; MRI, magnetic resonance imaging; NMLE, non-mass-like enhancement; sample-cores, all of sampled cores by needle biopsy; cancer-cores, cores containing cancer nests; HER2, human epidermal growth factor 2.

Table 2. Comparison of MRI findings and clinicopathological factors between pure DCIS and IBC groups in NMLE type

Variables	DCIS ($n = 49$)	IDC ($n = 11$)	P value (univariate)	P value (multivariate)
Age (years)			0.048	0.067
Median	55	44		
Range	34–76	39–66		
Physical examination			0.074	
Positive	4	3		
Negative	45	9		
Lesion size on MRI (mm)			0.018	0.027
Median	16	34		
Range	5–60	6–59		
Distribution			0.947	
Focal	8	2		
Linear	1	0		
Ductal	18	3		
Segmental	19	6		
Regional/multiple/diffuse	3	0		
Internal enhancement			0.601	
Homogeneous	2	0		
Heterogeneous	20	7		
Stippled, punctate	12	1		
Clumped	12	2		
Reticular, dendritic	3	1		
Initial-phase kinetic pattern			0.361	
Rapid	21	7		
Medium	24	4		
Slow	4	0		
Delayed-phase kinetic pattern		0.636		
Persistent	24	4		
Plateau	24	7		
Washout	1	0		
Signal intensity ratio			0.001	0.032
Median	1.35	2.01		
Range	1.04–2.89	1.56–2.55		
Type of biopsy procedure			0.929	
Core-needle biopsy	26	6		
Vacuum-assisted biopsy	23	5		
The number of sample-cores		0.724		
Median	5	4		
Range	2–12	1–13		
The number of cancer-cores			0.005	0.012
Median	3	2		
Range	1–10	1–7		
Nuclear grade			0.799	
1 (low)	38	9		
2 (intermediate)	6	1		

Continued

Table 2. *Continued*

Variables	DCIS ($n = 49$)	IDC ($n = 11$)	P value (univariate)	P value (multivariate)
3 (high)	5	1		
Comedo necrosis			0.606	
Positive	27	7		
Negative	22	4		
Estrogen receptor status			0.618	
Positive	39	8		
Negative	10	3		
Progesteron receptor status			0.610	
Positive	35	7		
Negative	14	4		
HER2 status			0.133	
Positive	8	4		
Negative	41	7		

Mass; $P = 0.022$), the number of cancer-cores ($P = 0.002$) and the findings on physical examination ($P = 0.021$).

Factors Associated with Invasive Disease in NMLE Type on MRI

In 60 cases classified as NMLE type on MRI, 49/60 (82%) were diagnosed as DCIS and 11/60 (18%) were diagnosed as IBC. The median lesion size on MRI in 11 IBC cases was 34 (range: 6–59) mm. This was statistically significantly larger than the median size of the 49 DCIS lesions (median: 16, range: 5–60 mm, $P = 0.018$, Table 2). On the other hand, there were no statistically significant differences between the two groups regarding the morphological features or kinetic patterns on dynamic study. The SI ratio of the IBC cases (median: 2.01, range: 1.56–2.55) represented a higher value than that of the DCIS cases (median: 1.35, range: 1.04–2.89), and the difference was the most statistically significant ($P = 0.001$, Table 2).

In the 32 cases preoperatively diagnosed by core-needle biopsy, six cases (19%) were finally diagnosed as IBC. In the 28 cases preoperatively diagnosed by vacuum-assisted biopsy, five cases (18%) were IBC. The detection rates of IBC were not significantly different between the type of biopsy procedures, core-needle biopsy and vacuum-assisted biopsy (Table 2). In relation to the clinicopathological factors, the number of cancer-cores was significantly associated with the final histological diagnosis, either DCIS (median: 3, range: 1–10) or IBC (median: 2, range: 1–7, $P = 0.005$, Table 2); however, the number of sample-cores was not significant. The other histological factors, namely NG, CN, ER, PgR and HER2, of the IBC cases did not differ from those of the DCIS cases. Additionally, the IBC patients (median: 44, range: 39–66) were younger than the DCIS patients (median: 55, range: 34–76, $P = 0.048$, Table 2).

The variables significantly associated with the upstage to IBC were examined with a multivariate analysis using a logistic-regression model. The results showed that lesion size on MRI ($P = 0.027$), the SI ratio ($P = 0.032$) and the number of cancer-cores ($P = 0.012$) were each independently correlated with the presence of invasive disease (Table 2). In addition, ROC and several statistical analyses were performed for these independent factors. The area under the curve was 0.72 for lesion size on MRI, 0.92 for the SI ratio and 0.80 for the number of cancer-cores (Table 3). The results of sensitivity, specificity, positive and negative predictive value and positive and negative likelihood ratios are listed in Table 3 at the cutoff value defined by ROC analyses. Among these three factors, the SI ratio was the most accurately correlated with the presence of invasive disease. There was only one IBC in the NMLE cases with lower SI ratio at a cutoff value 1.76.

Factors Associated with Invasive Disease in Mass Type on MRI

All the 15 cases classified as Mass type on MRI were preoperatively diagnosed by core-needle biopsy. Of them, 8/15 (53%) were diagnosed as DCIS and 7/15 (47%) were diagnosed as IBC. In this type, there were no statistically significant differences between the DCIS and IBC cases in terms of lesion size (median: 12, range: 5–31 versus median: 13, range: 6–18, $P = 0.642$), the SI ratio (median: 1.68, range: 1.11–2.66 versus median: 1.79, range: 1.54–2.23, $P = 0.679$), morphological features and kinetic patterns on MRI study. Similarly, age (median: 63, range: 41–70 versus median: 61, range: 46–71, $P = 0.825$) and histopathological

Table 3. The statistical results of the predictive factors in multivariate analysis for NMLE type

Variables	AUC	Cutoff value	Sensitivity (%)	Specificity (%)	PPV (%)	NPV (%)	PLR	NLR
Lesion size on MRI (mm)	0.72	31	64	84	47	92	3.90	2.30
Signal intensity ratio	0.92	1.76	91	88	63	98	7.42	8.78
The number of cancer-cores	0.80	2	82	80	47	95	4.01	4.38

AUC, area under the curve; PPV, positive predictive value; NPV, negative predictive value; PLR, positive likelihood ratio; NLR, negative likelihood ratio.

factors were not different between the two groups. While the numbers of sample-cores and cancer-cores were significantly smaller in the IBC cases (median: 2, range: 1–3 for both) than in the DCIS cases (median: 3, range: 2–5 for both, $P = 0.035$ and $P = 0.009$, respectively, Table 4), these variables were not found to be statistically independent in the multivariable analysis.

Comparison of the SI Ratios of the Non-invasive and Invasive Components of the IBC Cases

We could assess the SI ratios of the portions of the non-invasive and invasive components separately in 15 of the 18 IBC cases in which the cancerous lesions could be divided into the two different portions on MRI (Fig. 1). The SI ratios of the invasive component (median: 2.01, range: 1.56–2.55) were statistically significantly higher than those of the non-invasive component (median: 1.70, range: 1.51–2.02) in eight NMLE cases ($P = 0.029$, Fig. 2). Furthermore, the SI ratios of the invasive and non-invasive components represented significantly higher values than those of the 49 pure DCIS cases classified as NMLE type ($P = 0.001$ and $P = 0.034$, respectively, Fig. 2). In the Mass cases, there were no significant differences between the SI ratios of eight pure DCIS cases, the invasive component (median: 1.79, range: 1.54–2.23) and non-invasive component (median: 1.61, range: 1.31–1.86) in seven IBC cases (Fig. 2).

DISCUSSION

The surgical staging of axillary lymph nodes is unnecessary for pure DCIS patients; however, 8–38% of preoperatively diagnosed DCIS cases have been reported to have invasive disease in surgical specimens and should undergo SLNB (1–9). Therefore, accurately predicting occult invasion is so meaningful for clinicians to select which patients should undergo SLNB and to reduce the complications created by surgery as possible. Our study indicated that MRI findings, including the lesion size and SI ratio, and the number of cancer-cores, are significantly correlated with IBC in needle-biopsy-proven DCIS with NMLE type (Tables 2 and 3). Therefore, we suggest that DCIS without these associated factors with invasion could go on to surgery without SLNB and that DCIS with these factors should undergo SLNB at the time of surgery. In contrast, in Mass type, there were no independently significant variables of MRI and histopathology. These results might be affected by the small size of Mass cases (Table 4).

Previous studies have reported the usefulness of MRI with high spatial resolutions for detecting DCIS and accurately depicting the extent of diseases (10–14). These advances in imaging play important roles in the management of DCIS patients; however, the specific features of MRI that are associated with the upstage to IBC in preoperatively diagnosed DCIS are not yet clearly described. Typically, DCIS has been reported to have a tendency to represent NMLE features according to BI-RADS MRI (12,16,17). In the present study, 49 of 60 NMLE (82%) were diagnosed as DCIS in the surgical specimens. In contrast, 7 of 15 Mass (47%) had invasion, and the proportion of DCIS with the two lesion types was significantly different (Table 1).

In NMLE of our study, lesion size on MRI was an independent variable for differentiating IBC from pure DCIS and the morphological and kinetic features were absolutely useless, consistent with the results of previous reports (18,19). These results showed the limitations of the BI-RADS MRI criteria in selecting IBC among biopsy-proven DCIS. On MRI, the morphological and kinetic features reflect the entire breast lesion, not only one part, and so are not thought to be affected by the presence of occult invasion. To achieve the goal of our study, we focused on local characteristics by analyzing SI on dynamic MRI, which reportedly had a potential role in this situation (19,20). The SI ratio was an independently significant predictor of invasion in our NMLE (Table 2). Some previous reports have suggested that inflammatory responses and angiogenesis are activated surrounding cancer nests once invasion occurs (1,7). It is thought that these environmental changes are expressed on MRI findings, and the analyses of MRI findings with angiogenic factors such as vascular endothelial growth factor are expected.

Additionally, there was a significant difference in the SI ratios of the non-invasive components of 8 IBC and 49 pure DCIS ($P = 0.034$). This result had a limitation, because the number of IBC was too small for statistical assessment. However, previous studies have found that angiogenesis is observed in pre-invasive breast lesions and the characteristics

Table 4. Comparison of MRI findings and clinicopathological factors between pure DCIS and IBC groups in Mass type

Variables	DCIS ($n = 8$)	IDC ($n = 7$)	P value
Age (years)			0.825
Median	63	61	
Range	41–70	46–71	
Physical examination			0.464
Positive	2	3	
Negative	6	4	
Lesion size on MRI (mm)			0.642
Median	12	13	
Range	5–31	6–18	
Shape			0.702
Round/oval	2	3	
Lobular	4	3	
Irregular	2	1	
Margin			0.333
Smooth	0	0	
Irregular	7	7	
Spiculated	1	0	
Enhancement			0.379
Homogeneous	3	1	
Heterogeneous	5	5	
Rim enhancement	0	1	
Initial-phase kinetic pattern			0.398
Rapid	4	5	
Medium	4	2	
Slow	0	0	
Delayed-phase kinetic pattern			0.583
Persistent	3	1	
Plateau	3	4	
Washout	2	2	
Signal intensity ratio			0.679
Median	1.68	1.79	
Range	1.11–2.66	1.54–2.23	
The number of sample-cores			0.035[a]
Median	3	2	
Range	2–5	1–3	
The number of cancer-cores			0.009[a]
Median	3	2	
Range	2–5	1–3	
Nuclear grade			0.294
1 (low)	7	5	
2 (intermediate)	1	1	
3 (high)	0	1	
Comedo necrosis			0.782
Positive	4	3	
Negative	4	4	
Estrogen receptor status			0.919
Positive	7	6	
Negative	1	1	
Progesterone receptor status			0.464
Positive	6	4	
Negative	2	3	
HER2 status			0.605
Positive	2	1	
Negative	6	6	

[a]These variables were not found to be statistically independent in the multivariable analysis.

of non-invasive components of IBC and pure DCIS are different (21–23). Potentially, these biological features may produce differences in MRI findings between these two groups and may be useful in predicting the presence of invasion in surrounding areas.

Some investigators have suggested that histopathological factors are correlated with invasion; however, the others, including our study, are not (1,4–7,9). This controversy may exist because needle biopsy specimens represent only a part of whole breast lesions with heterogeneous features. Therefore, sampling more breast lesions has been recommended in order to improve the accuracy of preoperative diagnoses and to reduce the underestimation by sampling error (1,3,5). Assessing the presence or absence of sampling error is thought to be vital for making a preoperative diagnosis and constructing a therapeutic strategy. However, in previous studies, there has been little discussion regarding the proportion of cores reliably containing cancer nests in all sampled cores. For this reason, we analyzed both the number of sample-cores and cancer-cores. In our NMLE, the number of cancer-cores had an independently significant correlation with the presence of invasion; however, the number of sample-cores was not significant. These results show that the proportion of cancer nests detected on needle biopsy is clinically important to judge whether underestimation exits. Hence, clinicians should confirm the status of needle biopsy.

This study has several limitations. First, the reliability of the results was insufficient because the design included a retrospective analysis of a relatively small number of eligible patients. Therefore, we are now planning the prospective validation study with larger sample sizes in order to confirm our results as a next step. Second, these cases were diagnosed using two different gauges of needle biopsies. In

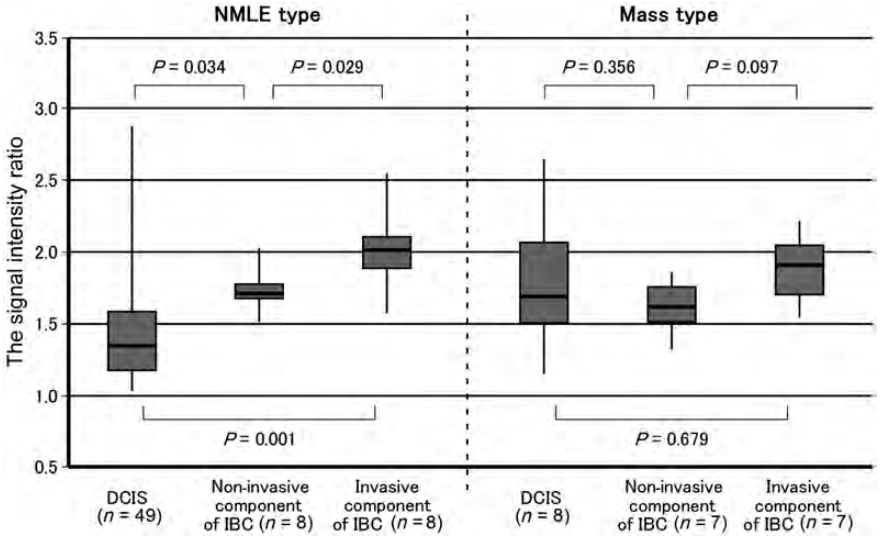

Figure 2. These graphs show the SI ratio as the SI of the detected lesion divided by that of the surrounding normal breast tissue in each lesion type on enhanced MRI. In non-mass-like enhancement (NMLE) type, the SI ratios of the invasive component of IBC ($n = 8$) were statistically significantly higher than those of the non-invasive component of IBC ($P = 0.029$). Furthermore, the SI ratios of the invasive and non-invasive components of IBC represented significantly higher values than those of pure ductal carcinoma *in situ* (DCIS, $n = 49$) with NMLE type ($P = 0.001$ and $P = 0.034$, respectively). In Mass type, there were no significant differences between the SI ratios of pure DCIS ($n = 8$), the invasive and non-invasive components of IBC ($n = 7$).

general, the detection rates of IBC were thought to be influenced by the gauge size of needle biopsies, and vacuum-assisted biopsy is the appropriate method for DCIS. However, the detection rates of IBC were not significantly different between the type of biopsy procedures, core-needle biopsy and vacuum-assisted biopsy in our study. We speculate that the results might be influenced by the selection bias that the cases with smaller and less obvious disease tended to undergo vacuum-assisted biopsy.

In conclusion, our study demonstrated that needle-biopsy-proven DCIS cases of NMLE type might be sufficiently managed using breast MRI features such as enhanced lesion size and SI, incorporating the number of cancer-cores at needle biopsy specimen in the clinical setting.

Conflict of interest statement

None declared.

References

1. Lee CH, Carter D, Philpotts LE, et al. Ductal carcinoma *in situ* diagnosed with stereotactic core needle biopsy: can invasion be predicted? *Radiology* 2000;217:466–70.
2. Cox CE, Nguyen K, Gray RJ, et al. Importance of lymphatic mapping in ductal carcinoma *in situ* (DCIS): why map DCIS? *Am Surg* 2001;67:513–9; discussion 519–521.
3. Jackman RJ, Burbank F, Parker SH, et al. Stereotactic breast biopsy of nonpalpable lesions: determinants of ductal carcinoma *in situ* underestimation rates. *Radiology* 2001;218:497–502.
4. Mittendorf EA, Arciero CA, Gutchell V, et al. Core biopsy diagnosis of ductal carcinoma *in situ*: an indication for sentinel lymph node biopsy. *Curr Surg* 2005;62:253–7.
5. Yen TW, Hunt KK, Ross MI, et al. Predictors of invasive breast cancer in patients with an initial diagnosis of ductal carcinoma *in situ*: a guide to selective use of sentinel lymph node biopsy in management of ductal carcinoma *in situ*. *J Am Coll Surg* 2005;200:516–26.
6. Goyal A, Douglas-Jones A, Monypenny I, et al. Is there a role of sentinel lymph node biopsy in ductal carcinoma *in situ*?: analysis of 587 cases. *Breast Cancer Res Treat* 2006;98:311–4.
7. Huo L, Sneige N, Hunt KK, et al. Predictors of invasion in patients with core-needle biopsy-diagnosed ductal carcinoma *in situ* and recommendations for a selective approach to sentinel lymph node biopsy in ductal carcinoma *in situ*. *Cancer* 2006;107:1760–8.
8. Moran CJ, Kell MR, Flanagan FL, et al. Role of sentinel lymph node biopsy in high-risk ductal carcinoma *in situ* patients. *Am J Surg* 2007;194:172–5.
9. Tan JC, McCready DR, Easson AM, et al. Role of sentinel lymph node biopsy in ductal carcinoma-*in situ* treated by mastectomy. *Ann Surg Oncol* 2007;14:638–45.
10. Lehman CD. Magnetic resonance imaging in the evaluation of ductal carcinoma *in situ*. *J Natl Cancer Inst Monogr* 2010;2010:150–1.
11. Berg WA, Gutierrez L, NessAiver MS, et al. Diagnostic accuracy of mammography, clinical examination, US, and MR imaging in preoperative assessment of breast cancer. *Radiology* 2004;233:830–49.
12. Menell JH, Morris EA, Dershaw DD, et al. Determination of the presence and extent of pure ductal carcinoma *in situ* by mammography and magnetic resonance imaging. *Breast J* 2005;11:382–90.
13. Kuhl CK, Schrading S, Bieling HB, et al. MRI for diagnosis of pure ductal carcinoma *in situ*: a prospective observational study. *Lancet* 2007;370:485–92.
14. Amano G, Ohuchi N, Ishibashi T, et al. Correlation of three-dimensional magnetic resonance imaging with precise histopathological map concerning carcinoma extension in the breast. *Breast Cancer Res Treat* 2000;60:43–55.
15. American College of Radiology. Breast Imaging Reporting and Data System (BI-RADS)-MRI atlas. Reston, VA: American College of Radiology 2003.
16. Jansen SA, Newstead GM, Abe H, et al. Pure ductal carcinoma *in situ*: kinetic and morphologic MR characteristics compared with mammographic appearance and nuclear grade. *Radiology* 2007;245:684–91.
17. Rosen EL, Smith-Foley SA, DeMartini WB, et al. BI-RADS MRI enhancement characteristics of ductal carcinoma *in situ*. *Breast J* 2007;13:545–50.

18. Kuhl C. The current status of breast MR imaging. Part I. Choice of technique, image interpretation, diagnostic accuracy, and transfer to clinical practice. *Radiology* 2007;244:356–78.
19. Goto M, Yuen S, Akazawa K, et al. The role of breast MR imaging in pre-operative determination of invasive disease for ductal carcinoma *in situ* diagnosed by needle biopsy. *Eur Radiol* 2011;22:1255–64.
20. Yuen S, Uematsu T, Kasami M, et al. Breast carcinomas with strong high-signal intensity on T2-weighted MR images: pathological characteristics and differential diagnosis. *J Magn Reson Imaging* 2007;25:502–10.
21. Ma XJ, Salunga R, Tuggle JT, et al. Gene expression profiles of human breast cancer progression. *Proc Natl Acad Sci USA* 2003;100:5974–9.
22. Schuetz CS, Bonin M, Clare SE, et al. Progression-specific genes identified by expression profiling of matched ductal carcinomas *in situ* and invasive breast tumors, combining laser capture microdissection and oligonucleotide microarray analysis. *Cancer Res* 2006;66:5278–86.
23. Wiechmann L, Kuerer HM. The molecular journey from ductal carcinoma *in situ* to invasive breast cancer. *Cancer* 2008;112:2130–42.